

Stabilized fiber-optic Mach–Zehnder interferometer for carrier-frequency rejection

Nathan Cooper,* Jonathan Woods, James Bateman,
Alexander Dunning, and Tim Freearge

School of Physics and Astronomy, University of Southampton, Highfield, Southampton SO17 1BJ, UK

*Corresponding author: nlc2g09@soton.ac.uk

Received 9 May 2013; revised 1 July 2013; accepted 1 July 2013;
posted 17 July 2013 (Doc. ID 190334); published 7 August 2013

We have demonstrated stabilization of a fiber-optic Mach–Zehnder interferometer, with a centimeter-scale path difference, to the transmission minimum for the carrier wave of a frequency-modulated laser beam. A time-averaged extinction of 32 dB, limited by the bandwidth of the feedback, was maintained over several hours. The interferometer was used to remove the carrier wave from a 780 nm laser beam that had been phase modulated at 2.7 GHz. © 2013 Optical Society of America

OCIS codes: (140.3298) Laser beam combining; (020.0020) Atomic and molecular physics; (020.2930) Hyperfine structure; (060.2310) Fiber optics.

<http://dx.doi.org/10.1364/AO.52.005713>

1. Introduction

Radio-frequency modulation allows the frequency precision of a stabilized laser to be coherently translated to adjacent wavelengths and pairs of optical frequencies to be generated with low differential frequency noise. When achieved by electro-optic modulation or direct modulation of the current through a diode laser, however, the different frequencies continue to propagate in the same beam mode. Spatial separation hence requires a frequency-dependent transmission or deflection. A commonly used device for this is the Mach–Zehnder interferometer (MZI): with an appropriate path difference within the device, the sidebands emerge from one output port and the carrier from the other. For certain wavelengths, a similar effect can be achieved by employing the frequency-dependent Faraday effect in an atomic vapor [1].

MZIs find applications as filters and frequency-dependent beam splitters and combiners [2] for a variety of applications in optics [3], metrology [4],

and quantum information [5]. Fiber-optic interferometers offer several advantages over free-space devices, such as improved output beam quality, easier integrability with other fiber-optic systems, lower sensitivity to vibrations and air currents, and a generally higher extinction ratio thanks to the ease and accuracy with which the beams may be recombined. Previous applications have included passively stable microscopic devices for refractive index measurement [6], interferometers that intentionally remain unstabilized for sensing purposes [4,7], and devices that have been actively stabilized by dithering [8,9] or locking to the side of an interference fringe [10]. Polarization-dependent methods such as Hänsch–Couillaud locking, which we have previously used to stabilize a free-space interferometer [11], cannot easily be applied to fiber-optic devices because of the high temperature dependence of the birefringence upon which polarization-maintaining fibers depend. Here, we demonstrate a similarly robust alternative stabilization method that is suitable for fiber-based interferometers, using a convenient variation of frequency-modulation stabilization [12].

2. Interferometer Stabilization

The stabilization of an interferometer to maximize or minimize the transmission at a given wavelength presents the difficulty that a deviation to either side of the optimum configuration has the same effect upon the transmitted intensity; this parameter itself therefore gives no indication of the sign of the correction required. One solution is to perturb the interferometer in a slow, periodic “dither” and monitor the relative phase of variation of the transmitted intensity. A popular alternative is to accept a small offset and stabilize the transmitted intensity to a value just below its peak or above its minimum. In both cases, being near a turning point in the measured parameter, the interferometer must be significantly perturbed or displaced for a measurable signal to be obtained.

A more elegant technique commonly used for the spectroscopic stabilization of lasers and optical resonators is to generate sidebands at frequencies either side of the wavelength required and measure the differential effect upon these components. In contrast to the large, slow perturbations of a dither, these components may be generated by the weak but rapid variations of frequency or phase modulation. The system remains in its stabilized configuration, and most of the optical power remains at the desired wavelength. Phase-sensitive detection of the beat note in the transmitted intensity then yields the error signal directly [12].

Here, partly for practical expedience and to avoid parasitic amplitude modulation, we use a variation upon conventional frequency modulation stabilization and generate the sidebands by acousto-optic modulation of a fraction of the incident light, which we then direct backward through the interferometer via the spare output port of the instrument. Where true frequency modulation uses beating of the sidebands with the carrier to provide a periodic alternation between the two sidebands, we achieve this directly by using a suitably aligned chopper wheel: although somewhat inelegant, this approach allows a large sideband spacing while requiring only low-frequency detection circuitry. The derived error signal is used to control the temperature, and hence refractive index, of one arm of the interferometer via a thermoelectric cooler (TEC) upon which one of the fibers is mounted; it would alternatively be possible to stretch the fiber using a piezoelectric actuator, as in [8].

Our apparatus is shown schematically in Fig. 1. The MZI is a custom device supplied by OzOptics [13], with internal fiber arms 0.3 m long, one of which is attached to a TEC to regulate its temperature. An incident laser beam with frequency ω_0 bearing sidebands at ± 2.7 GHz is directed into port A of the MZI; the sidebands are intended to emerge from port D, while the rejected carrier should be sent to port C. A fraction of the incident beam is split off from the main path and sent to the acousto-optic modulator (AOM), which produces two spatially distinct beams

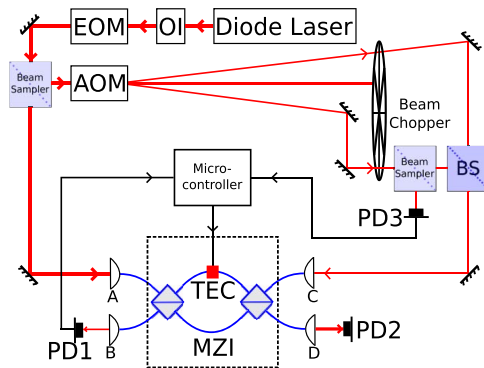


Fig. 1. Experimental setup of the MZI and surrounding optics. BS (beam splitter), AOM (acousto-optic modulator), OI (optical isolator), and TEC (thermoelectric cooler). Any of the light entering port A that emerges from port C is discarded, with unwanted feedback to the source laser being prevented by the optical isolator.

with frequencies $\omega_0 \pm \omega_{\text{AOM}}$, where $\omega_{\text{AOM}} \sim 2\pi \times 80$ MHz. These are alternately fed backwards through the interferometer to the photodiode PD1. Using an indication of the chopper wheel phase provided by PD3, a microcontroller determines the error signal, which is proportional to the difference in transmitted intensity between the two AOM beams and adjusts the current supplied to the TEC accordingly.

The error signal is given theoretically as follows. If the fiber lengths within the instrument are $l_0 \pm \Delta l/2$, and the fibers have a frequency-dependent refractive index $\eta(\omega)$ (including waveguide dispersion), then the accrued phase difference $\delta(\omega)$ between the two paths will be

$$\delta(\omega) = \omega \eta(\omega) \Delta l / c, \quad (1)$$

and the difference in phase difference $\Delta\delta$ between optical frequencies ω_0 and $\omega_0 + \omega_m$ will hence be

$$\begin{aligned} \Delta\delta(\omega_m) &= \delta(\omega_0 + \omega_m) - \delta(\omega_0) \\ &= (\Delta l / c) [(\omega_0 + \omega_m) \eta(\omega_0 + \omega_m) - \omega_0 \eta(\omega_0)], \quad (2) \end{aligned}$$

which may be expanded, assuming constant dispersion, to give

$$\begin{aligned} \Delta\delta(\omega_m) &\approx \frac{\Delta l}{c} \left[\omega_m \eta(\omega_0) + \omega_0 \frac{d\eta}{d\omega} \omega_m \right] \\ &= \frac{\Delta l \omega_m}{c} \left[\eta(\omega_0) + \omega_0 \frac{d\eta}{d\omega} \right] = \frac{\pi \omega_m}{\omega_s}, \quad (3) \end{aligned}$$

where ω_s is the difference between frequencies that will be separated by the interferometer and is given by

$$\omega_s = \frac{\pi c}{\Delta l \left[\eta(\omega_0) + \omega_0 \frac{d\eta}{d\omega} \right]}. \quad (4)$$

The fraction of light transmitted between diagonally opposite ports of the interferometer will then

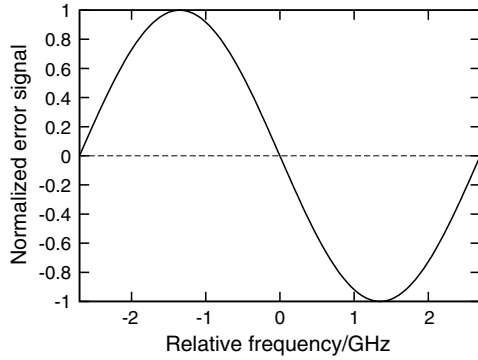


Fig. 2. Theoretical form of the error signal as a function of the difference in frequency between the (unshifted) input light and an optical frequency that would minimize T_{AD} , with $\omega_{AOM}/2\pi = 80$ MHz and $\omega_s/2\pi = 2.7$ GHz. Note that as $\omega_{AOM} \ll \omega_s$, the error signal closely approximates a sinusoid.

be proportional to $|1 + e^{i\delta(\omega)}|^2$, and the error signal will hence be proportional to

$$|1 + e^{i\delta(\omega_0 + \omega_{AOM})}|^2 - |1 + e^{i\delta(\omega_0 - \omega_{AOM})}|^2, \quad (5)$$

where $\delta(\omega \pm \omega_{AOM}) = \delta(\omega_0) \pm \Delta\delta(\omega_{AOM})$ as defined in Eq. (3) above. The form of the error signal E_s is hence given by

$$E_s \propto |1 + e^{i(\delta(\omega_0) + \pi\omega_{AOM}/\omega_s)}|^2 - |1 + e^{i(\delta(\omega_0) - \pi\omega_{AOM}/\omega_s)}|^2. \quad (6)$$

This is equal to zero and has finite gradient at both $\delta(\omega_0) = 0$ and $\delta(\omega_0) = \pi$. It is therefore suitable for stabilizing the interferometer to maximize transmission of the carrier to either output port according to the sign of the feedback [14]. A plot of this signal as a function of the frequency of the input beam is shown in Fig. 2.

3. Experiment and Results

A. Carrier Removal from a Phase-Modulated Spectrum

The separation of two closely spaced frequency components of a phase-modulated laser beam is a function that is often required in atomic physics experiments [15] and laser stabilization schemes [16]. For our atomic physics experiments, for example, in which we stimulate Raman transitions between the ground hyperfine states of ^{85}Rb , we modulate a 780 nm laser beam by passage through a 2.7 GHz electro-optic phase modulator (the remaining 300 MHz being provided by subsequent acousto-optic modulation), giving the spectrum shown in Fig. 3(a), in which 15% of the power is split between the two first-order sidebands. For use in our experiments, the central carrier must be largely eliminated. Many previous solutions incur a significant power loss [17] or offer only a limited extinction ratio [9].

The MZI allows the efficient separation of components that differ in frequency by an odd multiple of ω_s defined in Eq. (4). With an optical path difference $\eta\Delta l$ specified for our device as 56.0 ± 0.5 mm,

$\omega_s = 2.7$ GHz, and we may reject the carrier and send only the sidebands to the chosen output port of our interferometer, resulting in the spectrum shown in Fig. 3(b) in which the carrier has been suppressed by over 30 dB through interferometric means. In addition to this, the carrier and sidebands are both attenuated by 4 dB by passage through the interferometer, owing to the poor beam quality of the incident light which limited the coupling efficiency into the interferometer. Although a path difference tolerance was specified for the practical device, no measurable difference was found between the positions of minimum carrier transmission and maximum transmission of the first-order sidebands.

B. Feedback Stabilization of the Interarm Path Difference

The system in Fig. 1 was constructed, and the signals from each photodiode were sent to a simple digital control system based around an Arduino microcontroller [18]. The interferometer itself was constructed to our specifications by OzOptics [13], with the interarm path difference set such that $\omega_s = 2\pi \times 2.7$ GHz. Although our specifications allowed small inequalities in power division at the beam splitters, we in practice observe no measurable effects. With the input at port A and a constant total laser power, the signal from photodiode PD2 can be used to derive

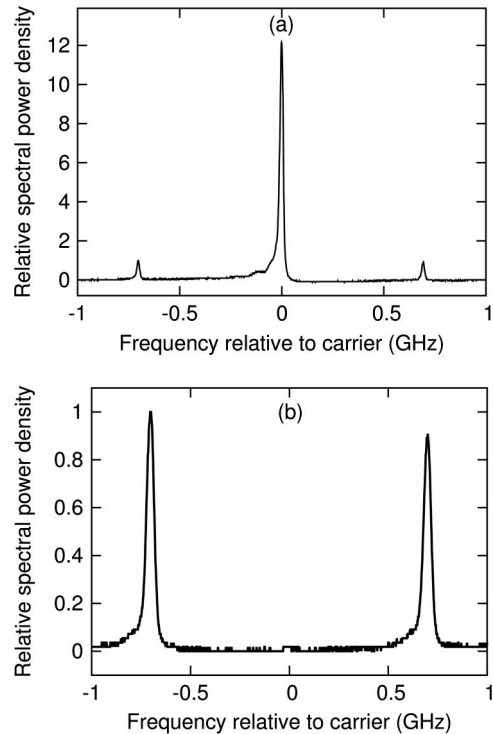


Fig. 3. Spectra of phase-modulated light (a) before and (b) after being passed through the interferometer while it was at a position of minimum carrier transmission to the relevant output. The modulation frequency is 2.7 GHz, and our spectrum analyzer is based on a cavity with a free spectral range of 2 GHz, hence, the apparent appearance of the first-order sidebands at ± 700 MHz relative to the carrier. Interferometric suppression of the carrier is in excess of 30 dB.

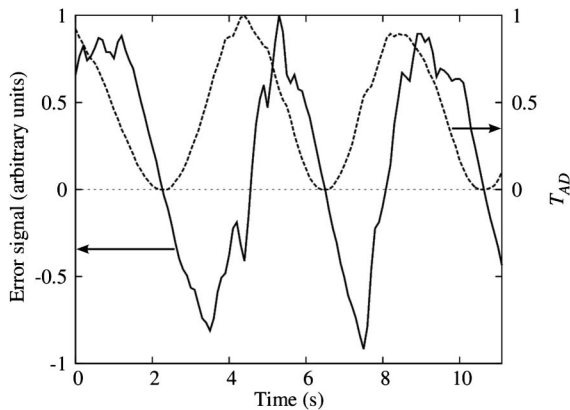


Fig. 4. Power transmission T_{AD} from port A to port D and error signal E_s shown as functions of time during a rapid scan of the interferometer over several fringes. The noise on the error signal is primarily electrical in origin.

the proportion T_{AD} of the optical power emerging from the interferometer's outputs that leave via port D. Equal powers must be coupled into the interferometer from each of the frequency-shifted beams entering port C; failure to do so results in narrowing of the locking region and a slight alteration of the lock point.

Figure 4 shows the variation of the power transmission T_{AD} and the error signal E_s during a rapid scan of the interarm path difference in the interferometer performed by making a sudden change to the current supplied to the TEC. The error signal not only exhibits a zero value corresponding with each minimum of T_{AD} but also the desired antisymmetric form about these points.

The power transmission T_{AD} was recorded for a period in excess of 2 h, during which the interferometer was actively locked to a minimum of T_{AD} (corresponding to $\delta_0 = \pi$). Fast Fourier transforms of $T_{AD}(t)$ over both this period and another period of equal

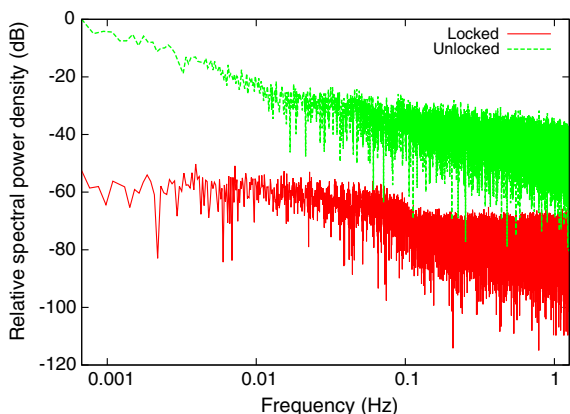


Fig. 5. Fast Fourier transforms of the measured values of $T_{AD}(t)$ over a period exceeding 2 h during which the interferometer was either actively stabilized at a minimum of T_{AD} ("locked" or lower trace) or allowed to drift freely ("unlocked" or upper trace). Spectral power density values are given relative to the maximum value measured, which was found at 0.674 mHz with the interferometer unlocked.

length during which the interferometer was left unstabilized are shown in Fig. 5. The time average of T_{AD} during this period was 6.3×10^{-4} (corresponding to an interferometric extinction of 32.0 dB). We believe this to have been limited by the response rate of our feedback system, as measurably nonzero values of T_{AD} were generally accompanied by a notable deviation of the error signal from zero. Extinction could therefore be improved by increasing the response rate of the feedback system, for example, by replacing the TEC with a fiber-stretching piezoelectric transducer, as in [8].

4. Conclusions

We have demonstrated a stable locking method for a fiber-optic MZI with a macroscopic interarm path difference. Our device allowed the time-averaged output from a chosen port to be interferometrically suppressed by 32 dB for a period of over 2 h. The extinction is believed to be limited by the response rate of our feedback system, which might be improved by switching from thermal to mechanical feedback. Our interferometer has been used to separate the carrier wave from the first-order sidebands of a 780 nm laser beam after electro-optic modulation at 2.7 GHz.

This work was supported by the UK EPSRC Grants No. EP/E039839/1 and EP/E058949/1.

References and Notes

1. R. Abel, U. Krohn, P. Siddons, I. Hughes, and C. Adams, "Faraday dichroic beam splitter for Raman light using an isotopically pure alkali-metal-vapor cell," *Opt. Lett.* **34**, 3071–3073 (2009).
2. D. Haubrich, "Lossless beam combiners for nearly equal laser frequencies," *Rev. Sci. Instrum.* **71**, 338–340 (2000).
3. A. de Vreede, M. Smit, B. Verbeek, E. Metaal, and F. Green, "Mach-Zehnder interferometer polarization splitter in InGaAsP/InP," *IEEE Photon. Technol. Lett.* **6**, 402–405 (1994).
4. P. Lu, L. Men, K. Sooley, and Q. Chen, "Tapered fiber Mach-Zehnder interferometer for simultaneous measurement of refractive index and temperature," *Appl. Phys. Lett.* **94**, 131110 (2009).
5. A. Ekert, J. Rarity, P. Tapster, and G. Palma, "Practical quantum cryptography based on two-photon interferometry," *Phys. Rev. Lett.* **69**, 1293–1295 (1992).
6. Y. Wang, M. Yang, D. N. Wang, S. Liu, and P. Lu, "Fiber in-line Mach-Zehnder interferometer fabricated by femtosecond laser micromachining for refractive index measurement with high sensitivity," *J. Opt. Soc. Am. B* **27**, 370–374 (2010).
7. T. Okamoto and I. Yamaguchi, "Multimode fiber-optic Mach-Zehnder interferometer and its use in temperature measurement," *Appl. Opt.* **27**, 3085–3087 (1988).
8. P. Connes and F. Reynaud, "Fiber tests on a radiotelescope," in *ESO Conference Workshop Proceedings*, Garching, Germany, no. 29 (1988), pp. 1117–1129.
9. I. Dotsenko, W. Alt, S. Kuhr, D. Schrader, M. Muller, Y. Miroshnychenko, V. Gomer, A. Rauschenbeutel, and D. Meschede, "Application of electro-optically generated light fields for Raman spectroscopy of trapped cesium atoms," *Appl. Phys. B* **78**, 711–717 (2004).
10. G. B. Xavier and J. P. von der Weid, "Stable single-photon interference in a 1 km fiber-optic Mach-Zehnder interferometer with continuous phase adjustment," *Opt. Lett.* **36**, 1764–1766 (2011).
11. J. E. Bateman, R. L. D. Murray, M. Himsworth, H. Ohadi, A. Xuereb, and T. Freearge, "Hänsch-Couillaud locking of

Mach–Zehnder interferometer for carrier removal from a phase-modulated optical spectrum,” *J. Opt. Soc. Am. B* **27**, 1530–1533 (2010).

12. R. Drever, J. Hall, F. Kowalski, J. Hough, G. Ford, A. Munley, and H. Ward, “Laser phase and frequency stabilisation using an optical resonator,” *Appl. Phys. B* **31**, 97–105 (1983).
13. www.ozoptics.com.
14. In our experiment, the light used to generate the locking signal was taken from the laser beam before the electro-optic phase modulator and hence contained only a single frequency component. If instead the sidebands are generated, for example, by modulation of the laser supply current, they will remain present in the monitor beam and could lead to additional features and false lock points. However, provided that the sidebands are separated from the carrier by integer multiples of ω_s , they will merely change the magnitude of the error signal and not alter its form, although in the case of strong modulation, the sign of the error signal may be reversed.
15. N. Davidson, H. J. Lee, M. Kasevich, and S. Chu, “Raman cooling of atoms in two and three dimensions,” *Phys. Rev. Lett.* **72**, 3158–3161 (1994).
16. J. I. Thorpe, K. Numata, and J. Livas, “Laser frequency stabilization and control through offset sideband locking to optical cavities,” *Opt. Express* **16**, 15980–15990 (2008).
17. N. Cooper, J. Bateman, A. Dunning, and T. Freearge, “Actively stabilized wavelength-insensitive carrier elimination from an electro-optically modulated laser beam,” *J. Opt. Soc. Am. B* **29**, 646–649 (2012).
18. We used an Arduino Uno board (<http://www.arduino.cc>), an electronics prototyping platform employing an Atmel ATMEGA328P-PU microprocessor. Buffered by an additional field effect transistor, this regulated the TEC duty cycle using 12 bit pulse-width modulation.